

LAYERWISE FINITE ELEMENT FOR FREE VIBRATION ANALYSIS OF GEOMETRICALLY IMPERFECT FGM PLATES

SLOJEVITI KONAČNI ELEMENT ZA ANALIZU SLOBODNIH VIBRACIJA FGM PLOČA SA PRISUSTVOM GEOMETRIJSKIH IMPERFEKCIJA

Originalni naučni rad / Original scientific paper
 Rad primljen / Paper received: 14.04.2026
<https://doi.org/10.69644/ivk-2026-02-0205>

Adresa autora / Author's address:
 University of Belgrade, Faculty of Civil Engineering, Belgrade,
 Serbia M. Četković <https://orcid.org/0000-0001-8595-0424>
 email: cetkovicm@grf.bg.ac.rs

Keywords

- free vibration
- FGM plate
- geometrical imperfections
- finite element

Abstract

The paper presents for the first time the finite element solution for free vibration response of a geometrically imperfect FGM plate based on layerwise theory of Reddy. The numerical solution is implemented in the original MATLAB[®] programme. The programme is used to analyse various parameters of importance for free vibration response. It is shown that free vibration response is sensitive to geometric parameters (a/h and b/a ratios), plate material gradation parameter (n), imperfection form and amplitude (μ), as well as boundary conditions. The presented results show close agreement with reference results from the literature and may serve for the future study of FGM based structures.

INTRODUCTION

One of the critical loading conditions, important for the safe design of structures is failure due to vibrations. Vibrations may be initiated from external source, or by initial disturbance, when no external force is applied. The first are forced vibrations, and the second are free vibrations. Both vibrations may be damped or undamped, linear or nonlinear [1]. In this paper, linear undamped free vibrations are analysed. The free vibration generally depends on structural geometry, material model, boundary/initial conditions, as well as on the presence of initial imperfections.

The initial imperfections often appear during the manufacturing process or in-service life, influencing the overall load capacity of the structure. They are classified into material or constructional imperfections and initial geometrical

Ključne reči

- slobodne vibracije
- FGM ploča
- geometrijske imperfekcije
- konačni element

Izvod

U ovom radu je po prvi put prikazan konačni element za analizu slobodnih vibracija FGM ploča sa geometrijskim imperfekcijama, zasnovan na Redijevoj slojevitoj teoriji ploča. Numeričko rešenje je primenjeno za sastavljanje originalnog programa u MATLAB[®] programskom jeziku. Programom su analizirani različiti parametri od značaja za slobodne vibracije ploče. Pokazuje se da slobodne vibracije zavise od geometrijskih parametara ploče (a/h i b/a), indeksa zapreminskog udela pojedinog materijala (n), oblika i amplitude imperfekcije (μ), kao i graničnih uslova ploče. Prikazani rezultati pokazuju blisko slaganje sa referentnim rezultatima iz literature i mogu se koristiti u budućoj analizi konstrukcija sačinjenih od FGM materijala.

imperfections. The initial geometrical imperfections include imperfections in loading mechanisms and imperfections in structural geometry. Imperfections in structural geometry have the tendency to increase or decrease natural frequencies, causing hardening or softening behaviour of the structure. In linear analysis, the hardening behaviour is typically present in perfect beam and plate-like structures. The increase of stiffness is caused by additional stretching of the middle surface. The softening behaviour is a characteristic for curved shells, where imperfection in shell curvature tend to 'flatten' its arch-like geometry. As a consequence of either hardening or softening behaviour, the resonance frequency of the structure changes. Namely, it shifts to the right in case of hardening, and to the left in case of softening response.

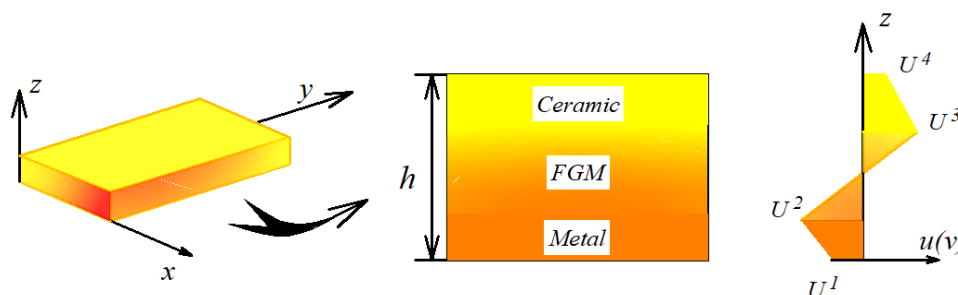


Figure 1. Geometry and displacement field of FGM plate.

However, in the geometrically nonlinear analysis, the response of structures in general is more complex, and it may change from softening to hardening behaviour, depending on imperfection size, imperfection form, or boundary conditions /2/. Most studies reported in literature assume the sinusoidal form of initial geometrical imperfection /3-7/. However, as concluded by Schneider et al. /8/, it is not possible to determine the most unfavourable shape of imperfection, since there is a dependency between the structural response (such as deflections, stresses, natural frequency or buckling loads) and the imperfection form and amplitude. Therefore, a need for the general form of imperfection is assumed in this study. Besides geometric imperfections, the free vibration response may be affected by the selection of material model.

Over the years, isotropic material models have a tendency to be replaced by composite material models. The composite material models usually have, either anisotropic homogeneous or isotropic nonhomogeneous behaviour. The representative of the first group are laminated composites or FRPs (Fibre Reinforced Polymer), while the representative of the second one are the FGMs (Functionally Graded Materials).

FGMs are defined as materials whose properties vary continuously in one or three directions. These gradual changes of material properties overcome the disadvantages of traditional FRP composites, regarding inter- and intra-laminar failure modes. FGMs are usually a mixture of two materials, for example metal and ceramic, where metal provides high toughness, while ceramics gives high thermal resistance /9/. Material properties of FGMs, often called effective material properties, are mathematically defined by specific homogenization scheme. The homogenization scheme assumes the definition of rule of mixture along with the volume fraction variation. The volume fraction variation may include Power law model (P-FGM), Exponential model (E-FGM), Sigmoid law model (S-FGM), or others. When the appropriate homogenization scheme is adopted, the mathematical formulation, numerical solution and finally the response of FGM structural components under various loading conditions may be found.

Mathematical models for free vibration analysis of FGM plates are formulated using either 3D theory of elasticity, Equivalent Single Layer theories (ESL), and more recently Carrera's Unified Formulation (CUF). Since there are a limited number of 3D elasticity solutions, the most in the literature for free vibrations of FGM plates are based on ESL theories, and a limited number of layerwise or zig-zag theories. The solutions to mathematical models are then given either by analytical or numerical solutions. Numerical solutions are most general, in terms of structural geometry and boundary conditions. The commonly used numerical solution is the finite element method (FEM). The FEM, as a core for most commercial software still remains the most exploited tool, apart from novel numerical methods, such as Isogeometric Analysis (IGA) or meshless methods, /10-13/.

The most reported solutions for free vibrations of FGMs are given using analytical methods. Viet Hoang et al. /14/ used new trigonometric shear deformation plate theory (TSDPT) and Galerkin's method for free vibration analysis

of two-directional variable thickness FGM plates resting on the Kerr elastic foundation. Foroughi et al. /15/ studied free vibration and buckling of FGM plates resting on elastic foundation, using quasi-3D higher-order shear deformation theory (HSDT). Governing equations of motion are solved using the finite strip method. Effects of parameters, such as plate thickness-to-length ratio, length-to-width ratio, boundary conditions, and the power-law index are analysed. Zhao et al. /16/ used higher-order shear deformation theory (HSDT) for free vibration and transient response of functionally graded porous (FGP) rectangular plates. Analytical solution is obtained using the combination of Jacobi-Ritz method and multi-segment strategy. Effects of porosity distribution, boundary conditions, elastic springs, plate geometry and dynamic load variation are studied. Demirhan et al. /17/ presented a Lévy-type solution for bending and free vibration of porous FG rectangular plates. They showed that porosity parameter and power-law index affect both bending and vibration response.

Ye et al. /18/ presented scaled finite element solution based on 3D elasticity theory for free vibration and bending analysis of P-FGM plates. The effect of different parameters, such as geometrical parameters (plate dimensions ratios and skew angle), power law indexes (n), and boundary conditions are considered, and a highly accurate solution is obtained. Katili et al. /19, 20/ investigated free vibration, bending and thermal buckling of FGM sandwich and skew plates using quadrilateral finite element with five degrees of freedom per node, based on improved FSDT (First order shear deformation theory). Belarbi et al. /21/ further included the effects of porosity distribution on free vibration, bending and buckling of P, S, E-FGM plates using C0 eight-node isoparametric Lagrangian quadrilateral element based on improved FSDT. The solution verified that the even porosity distribution gives the highest stiffness. Assas et al. /22/ used 4-node quadrilateral plate element, with six degrees of freedom at each node, based on improved FSDT to study bending, free vibration and stability of FGM plates, with various boundary conditions. Assas et al. /23/ further formulated four-node quadrilateral elements with five degrees of freedom per node based on the High-Order Shear Deformation Theory (HSDT) to study the static and free vibration of square, skew, and circular FG plates. Finally, Pham et al. /24/ extended previous finite element to analyse bending, free vibration and buckling of bi-directional in-plane FGM plates.

At authors' best knowledge, a finite element solution has not been reported for free vibration of geometrically imperfect FGM plates based on layerwise plate theory, /25/. Mathematical model assumes layerwise variation of in-plane displacements and constant transverse displacement through plate thickness, linear strain displacement relations with Koiter's imperfection model and linear elastic FGM material model. Material model is made of mixture metal and ceramic, with power law variation of volume fraction of ceramic constituent. After adopting the rule of mixture, the effective material properties of FGM plate are obtained. Hamilton's principle is used to derive the equation of motion for the free vibration problem. The solution is obtained using nine-node Lagrangian isoparametric finite element. The

numerical solution is incorporated into an original MATLAB programme which is used to perform the validation and parametric study. Effects of geometric parameters, such as side to thickness ratio (a/h), aspect ratio (b/a), power law index (n), material characteristics, imperfection amplitude (μ), imperfection form, and boundary conditions on vibration frequency are presented and are verified with the available results from literature.

MATHEMATICAL MODEL

Basic assumptions

The plate length and width along x and y directions are a and b , while plate thickness is h , with origin of coordinate system at the bottom surface of the plate. It is assumed that 1) material is isotropic and nonhomogeneous [26, 27] made of mixture metal and ceramics, 2) strains are small with Koiter's imperfection model, 3) material is linear elastic, and 4) inextensibility of normal is imposed.

Displacement field

In the LW theory of Reddy [25] in-plane displacements components (u, v) are interpolated through the thickness using 1D linear Lagrangian interpolation function $\Phi^I(z)$, while transverse displacement w is assumed to be constant through the thickness, Fig. 1:

$$\begin{aligned} u_1(x, y, z) &= u(x, y) + \sum_{I=1}^{N+1} U^I(x, y) \cdot \Phi^I(z), \\ u_2(x, y, z) &= v(x, y) + \sum_{I=1}^{N+1} V^I(x, y) \cdot \Phi^I(z), \\ u_3(x, y, z) &= w(x, y). \end{aligned} \tag{1}$$

Strain-displacement relations

The linear strain displacement relations with Koiter's imperfection model are assumed as:

$$\begin{aligned} \epsilon_{xx} &= \frac{\partial u}{\partial x} + \sum_{I=1}^{N+1} \frac{\partial U^I}{\partial x} \Phi^I + \frac{\partial w}{\partial x} \frac{\partial w_0}{\partial x}, \\ \epsilon_{yy} &= \frac{\partial v}{\partial y} + \sum_{I=1}^{N+1} \frac{\partial V^I}{\partial y} \Phi^I + \frac{\partial w}{\partial y} \frac{\partial w_0}{\partial y}, \\ \gamma_{xy} &= \frac{\partial u}{\partial y} + \frac{\partial v}{\partial x} + \sum_{I=1}^{N+1} \left(\frac{\partial U^I}{\partial y} + \frac{\partial V^I}{\partial x} \right) \Phi^I + \frac{\partial w}{\partial y} \frac{\partial w_0}{\partial x} + \frac{\partial w}{\partial x} \frac{\partial w_0}{\partial y}, \\ \gamma_{xz} &= \sum_{I=1}^{N+1} U^I \frac{d\Phi^I}{dz} + \frac{\partial w}{\partial x}, \\ \gamma_{yz} &= \sum_{I=1}^{N+1} V^I \frac{d\Phi^I}{dz} + \frac{\partial w}{\partial y}, \end{aligned} \tag{2}$$

where: w_0 is initial imperfection function, assumed in the following form:

$$w_0 = \mu \cdot h \cdot \operatorname{sech}[\delta_1(x/a - \psi_1)] \cdot \cos[\mu_1 \pi(x/a - \psi_1)] \cdot \operatorname{sech}[\delta_2(y/b - \psi_2)] \cdot \cos[\mu_2 \pi(y/b - \psi_2)], \tag{3}$$

where: μ represents the amplitude of imperfection that varies between 0 and 1; δ_1 and δ_2 are constants that define the localised degree of imperfection; while μ_1 and μ_2 are half wave numbers of the imperfection in the x and y axis, in respect.

A variety of imperfection forms, presented in Fig. 2, such as sine type, global type, and localised type, may be obtained by variation of parameters in Eq.(3).

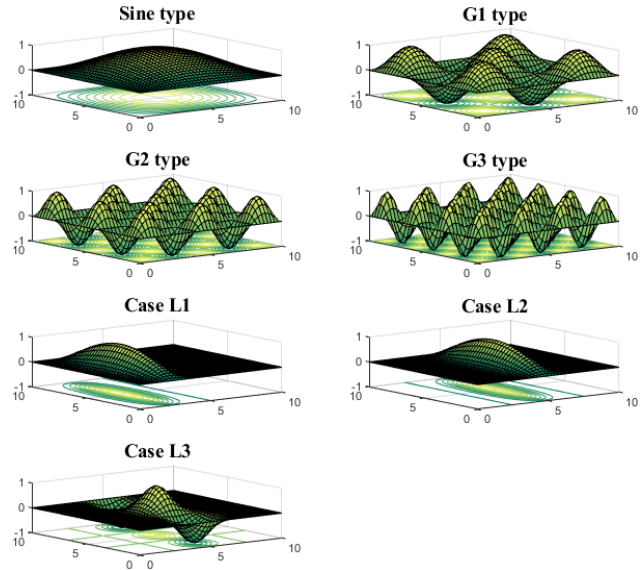


Figure 2. Geometric imperfection forms.

Constitutive equations

The plate is made from mixture of ceramic and metal, where the rule of mixture is defined as:

$$V_c + V_m = 1. \tag{4}$$

The volume fraction of ceramic is given by the power law distribution, in the thickness direction as (Fig. 3):

$$V_c(z) = \left(\frac{z}{h} \right)^n, \tag{5}$$

where: n denotes the power law index by which the gradation of constituents is controlled and may take values $[0, \infty]$.

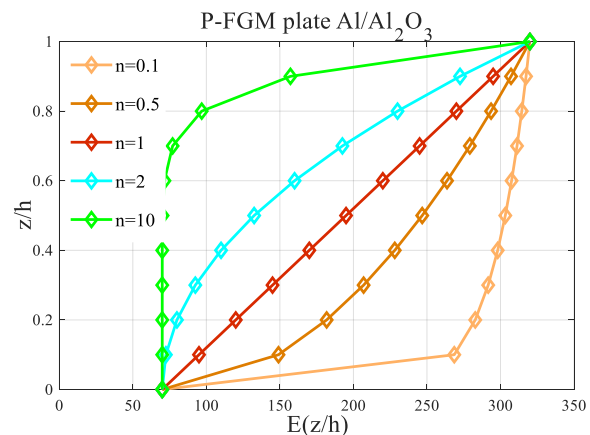


Figure 3. Young's modulus through the thickness of P-FGM Al/Al₂O₃ material model.

When the volume fraction exponent is 0, the plate is fully made of ceramic, and when the volume fraction exponent is 1, the variation of the volume fraction is linear. Then the effective material properties of FGM plate are:

$$P_e = P_m + (P_c - P_m)V_c(z), \tag{6}$$

such as Young's modulus $E(z)$ and mass density $\rho(z)$, while Poisson's coefficient ν is assumed to be constant. Subscripts m and c denote metal and ceramic, corresponding to the material property of the lower and upper surfaces of the plate, respectively.

With assumed strain displacement field, an isotropic non-homogeneous linear Hooke's material is used to formulate constitutive equations as:

$$\{\boldsymbol{\sigma}\} = [\mathbf{Q}] \cdot \{\boldsymbol{\varepsilon}\} \tag{7}$$

where: $\boldsymbol{\sigma} = \{\sigma_{xx} \sigma_{yy} \tau_{xy} \tau_{xz} \tau_{yz}\}^T$, $\boldsymbol{\varepsilon} = \{\varepsilon_{xx} \varepsilon_{yy} \gamma_{xy} \gamma_{xz} \gamma_{yz}\}^T$ are stress and strain components, respectively; while \mathbf{Q}_{ij} are elastic stiffness given as:

$$\begin{aligned} Q_{11} = Q_{22} &= \frac{(1-\nu)}{(1-2\nu)(1+\nu)} E(z), \\ Q_{12} = Q_{13} = Q_{23} &= \frac{1}{(1-2\nu)(1+\nu)} E(z), \\ Q_{33} = Q_{44} = Q_{55} &= \frac{1}{2(1+\nu)} E(z). \end{aligned} \tag{8}$$

Equilibrium equations

Using Hamilton's principle, the governing Euler-Lagrange equations of motion for free vibration of imperfect FGM plates are given in the following form:

$$\begin{aligned} N_{xx,x} + N_{xy,y} &= I_0 \ddot{u} + \sum_{J=1}^N I^J \ddot{U}^J, \\ N_{xy,x} + N_{yy,y} &= I_0 \ddot{v} + \sum_{J=1}^N I^J \ddot{V}^J, \\ Q_{x,x} + Q_{y,y} + N(w_0) &= I_0 \ddot{w}, \\ N_{xx,x}^I + N_{xy,y}^I - Q_{xz}^I &= I^I \ddot{u} + \sum_{J=1}^N I^{IJ} \ddot{U}^J, \\ N_{xy,x}^I + N_{yy,y}^I - Q_{yz}^I &= I^I \ddot{v} + \sum_{J=1}^N I^{IJ} \ddot{V}^J, \end{aligned} \tag{9}$$

where: ρ is mass density;

$$\begin{aligned} (I_0, I^I, I^{IJ}) &= \int_{-h/2}^{h/2} [\rho(z)(1, \Phi^I, \Phi^I \Phi^J)] dz; \\ N(w_0) &= N_{xx}^0(w_{0,xx}) + 2N_{xy}^0(w_{0,xy}) + N_{yy}^0(w_{0,yy}). \end{aligned}$$

FINITE ELEMENT MODEL

The weak form of governing Eq.(9) is discretised using eight node Lagrangian finite element. Over each element, the displacements are expressed as linear combination of shape functions and primary nodal variables:

$$\begin{aligned} \begin{Bmatrix} u \\ v \\ w \end{Bmatrix}^e &= \begin{Bmatrix} \sum_{j=1}^m u_j \Psi_j \\ \sum_{j=1}^m v_j \Psi_j \\ \sum_{j=1}^m w_j \Psi_j \end{Bmatrix}^e = \sum_{j=1}^m [\Psi_j]^e \{d_j\}^e, \\ \begin{Bmatrix} U^I \\ V^I \end{Bmatrix}^e &= \begin{Bmatrix} \sum_{j=1}^m U_j^I \Psi_j \\ \sum_{j=1}^m V_j^I \Psi_j \end{Bmatrix}^e = \sum_{j=1}^m [\bar{\Psi}_j]^e \{d_j^I\}^e, \end{aligned} \tag{10}$$

where: $\{d_j\}^e = \{u_j^e \ v_j^e \ w_j^e\}^T$; $\{d_j^I\}^e = \{U_j^I \ V_j^I\}^T$ are displacement vectors in the middle plane and the I -th plane, respectively; while $[\Psi_j]^e$, $[\bar{\Psi}_j]^e$ are interpolation function matrices for the j -th node of element Ω^e , given in /28/.

Substituting element displacement field Eq.(10) into weak form of governing Eq.(9), the finite element equations are obtained as:

$$([\mathbf{K}]^e + [\mathbf{K}_0]^e - \omega_{cr}^2 [\mathbf{M}]^e) \{\Delta\}^e = \{\mathbf{0}\}, \tag{11}$$

where: element stiffness matrix $[\mathbf{K}]^e$ and the element mass matrix $[\mathbf{M}]^e$ are given in /28/; while element initial stiffness matrix $[\mathbf{K}_0]^e$ is given in /29/.

Solution of Eq.(11) gives eigenvalues or vibration frequencies $\omega_1, \omega_2, \dots \omega_N$, and corresponding eigenvectors are free vibration mode shapes. The smallest of vibration frequencies not equal to zero is the critical frequency ω_{cr} and the corresponding eigenvector is first mode shape.

NUMERICAL RESULTS AND DISCUSSION

Using previous derived finite element solution, an original computer programme is coded using MATLAB® programming language, for free vibration of imperfect FGM plates. Element stiffness matrix, element mass and initial element stiffness matrix are evaluated using 3x3 Gauss-Legendre integration scheme for 2D quadratic in-plane interpolation, Fig. 4. The following boundary conditions at plate edges are used:

Simply supported: SSSS

$$\begin{cases} x=0, a: v_0 = w_0 = V^I = 0 \\ y=0, b: u_0 = w_0 = U^I = 0 \end{cases} \quad I=1, \dots, N+1$$

Clamped: CCCC

$$\begin{cases} x=0, a: u_0 = v_0 = w_0 = U^I = V^I = 0 \\ y=0, b: u_0 = v_0 = w_0 = U^I = V^I = 0 \end{cases} \quad I=1, \dots, N+1$$

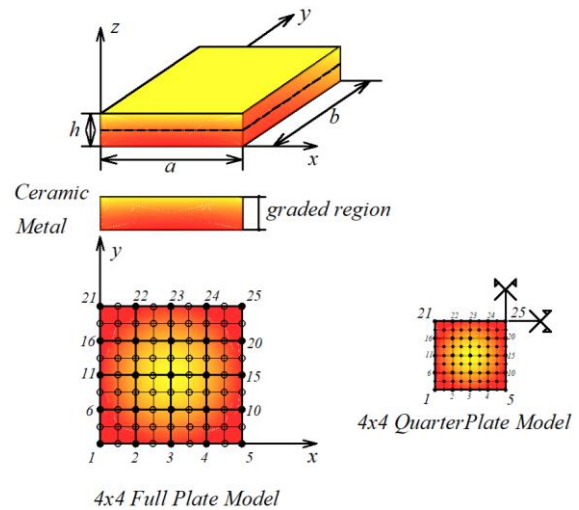


Figure 4. Plate finite element model.

Material properties are given in Table 1.

Table 1. Material properties.

	Ceramic		Metal		
Material	Al ₂ O ₃	ZrO ₂	Al	SUS304	Ti-6Al-4V
E (GPa)	380	151	70	201.4	105.7
ρ (kg/m ³)	3800	3000	2702	8166	4429
ν	0.3	0.3	0.3	0.3	0.3

Example 1: Influence of plate geometry

Free vibration mode shapes of perfect simply supported square metal-ceramic Al/Al₂O₃ plate, with $a/h = 10$ and $n = 1$, are presented in Fig. 5 and are compared with HSDT /30/ solutions from literature. It may be seen that the first and fourth modes are symmetric, while second and fourth modes are antisymmetric. Also, the vibration amplitude decreases with increase of vibration mode.

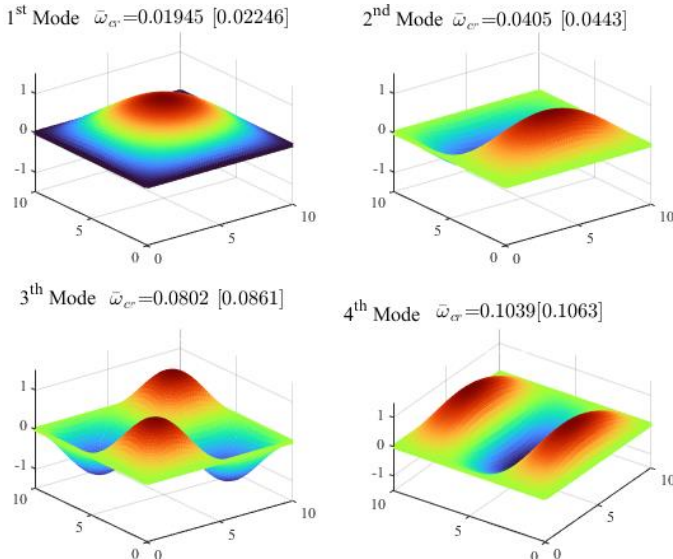


Figure 5. Free vibration mode shapes of simply supported Al/Al₂O₃ plate ($a/h = 10, n = 1$).

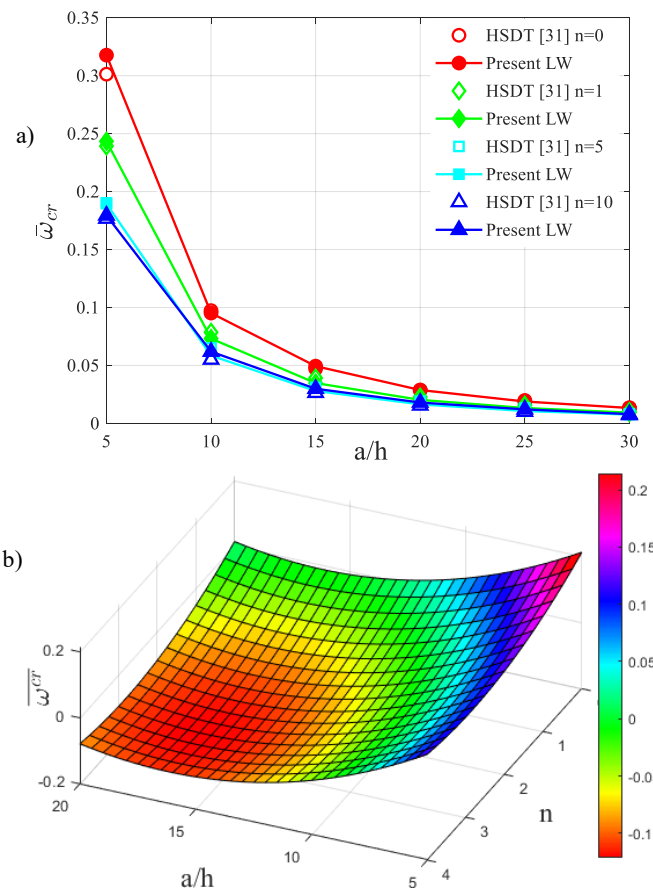


Figure 6. Nondimensional frequency: a) for different values of side to thickness ratio a/h ; b) surface for different values of $(a/h, n)$.

Influence of side to thickness ratio a/h on non-dimensional frequency $\omega_{cr} = \omega h \sqrt{(\rho_c/E_c)}$ is presented in Fig. 6a for simply supported Al/Al₂O₃ square plate and different values of power law index $n = 0, 1, 5,$ and 10 . The present results are compared with HSDT /31/ solutions from literature. It may be seen that for all power law index n , non-dimensional frequency decreases with the increase of side to thickness ratio a/h . This decrease is more severe for thick plates $a/h < 20$, as well for stiff ceramic plates, compared to FGM and metallic plates. Close agreement with results from /31/ is achieved. Additionally, non-dimensional frequency surface $\omega_{cr}(a/h, n)$ is presented in Fig. 6b in order to analyse the mutual influence of both side to thickness ratio a/h and power law index n . Obviously, the thickness variation a/h has shown greater impact on plate stiffness reduction, compared to power law index n .

A similar conclusion may be derived for the effect of aspect ratio b/a on non-dimensional frequency $\omega_{cr} = \omega h \sqrt{(\rho_c/E_c)}$ presented in Fig. 7a, of simply supported Al/ZrO₃ square plate /31/ ($a/h = 10$), with different values of power law index $n = 0, 1, 5,$ and 10 . The increase of aspect ratio b/a decreases non-dimensional frequency for all power law index n . The decrease is greater for $b/a < 2$. The close agreement with the results from /31/ is achieved. Additionally, non-dimensional frequency surface $\omega_{cr}(b/a, n)$ is presented in Fig. 7b. Again, the increase of aspect ratio b/a has shown greater impact on non-dimensional frequency, compared to increase of power law index n .

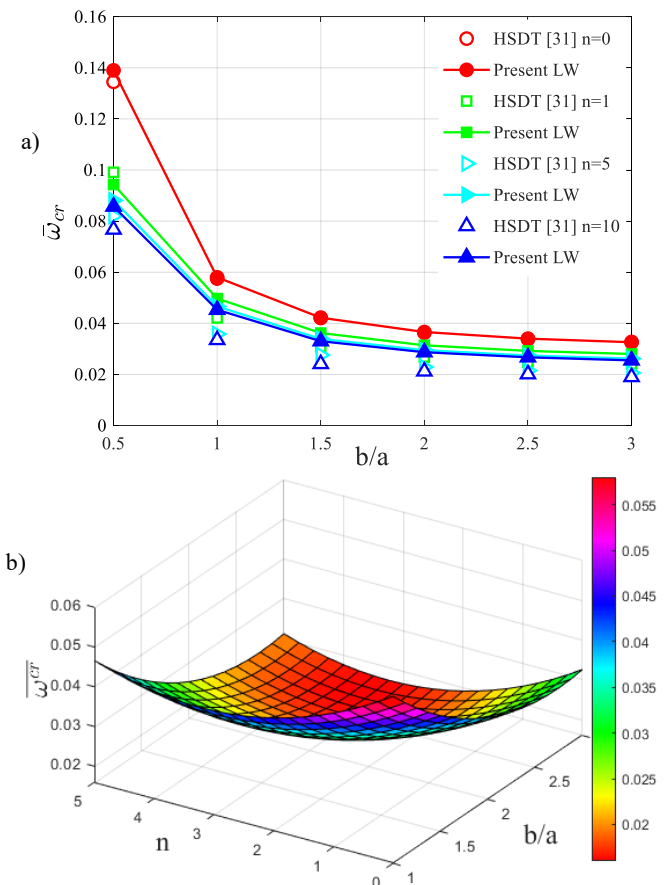


Figure 7. Nondimensional frequency: a) for different values of aspect ratio b/a ; b) surface for different values of $(b/a, n)$.

Example 2: Influence of material graduation

The influence of power law index n on non-dimensional natural frequency of simply supported Ti-6Al-4V/Al₂O₃ perfect plate /31/ for various side to thickness ratio a/h is presented in Fig. 8. The frequency is assumed in the following form $\omega_{cr} = \omega \sqrt{[12(1 - \nu^2)\rho_c a^2 b^2 / (\pi^4 E_c h^2)]}$. It is noticeable that as volume fraction index ranges from 0 to 10, the frequency parameter decreases. Namely, the larger volume fraction index assumes that the plate contains smaller amount of ceramic constituent, and thus the reduced stiffness.

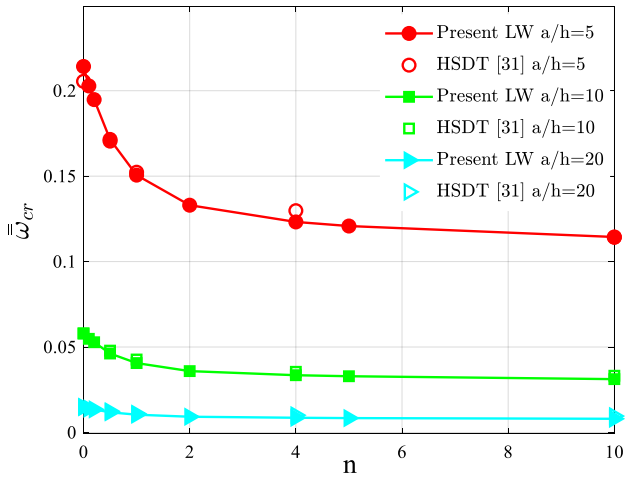


Figure 8. Non-dimensional frequency for different values of volume fraction ratio n .

Example 3: Influence of initial imperfection

The influence of imperfection form on free vibration frequency of ceramic Si₃N₄ plate ($a/b = 1$, $a/h = 10$) with $E = 322.2$ GPa, $\rho = 2370$ kg/m³, and $\nu = 0.3$ is presented in Fig. 9 as a function of imperfection amplitude μ . It is shown that L3 and L2 local-type imperfection forms have the least effect, while global-type imperfections G3, G2 and G1 have the greatest effect on free vibration frequency. This may be explained from the fact that as the imperfection form approaches the free vibration mode shape of the plate, the higher frequencies are expected. Also, it is shown that free vibration frequency increases with the increase of imperfection amplitude μ .

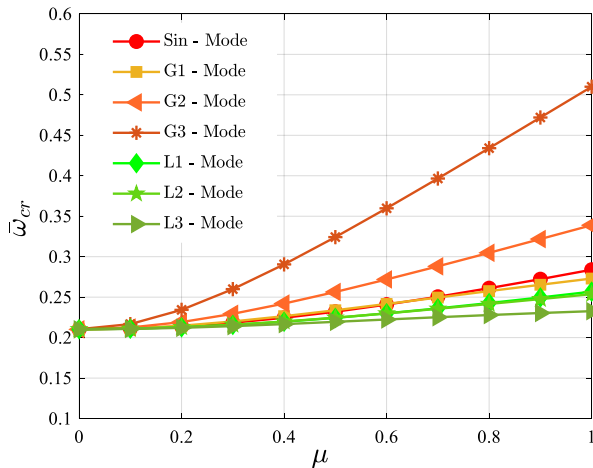


Figure 9. Free vibration frequency for different imperfection forms.

Example 4: Influence of boundary condition

The influence of boundary conditions on imperfect ceramic metal Si₃N₄/SUS304 plate with sinusoidal imperfection form $w_0 = \mu h \sin(\pi x/a) \sin(\pi y/b)$ are presented in Figs. 10a and 10b ($a/b = 1$, $a/h = 10$). It is shown that clamped plate in Fig. 10b has almost double free vibration frequency compared to simply supported plate /5/, in Fig. 10a. Also, the clamped plate has confirmed to be more sensitive to an increase of imperfection amplitude μ and ceramic volume fraction n . The reason is that both cases are with higher plate stiffness.

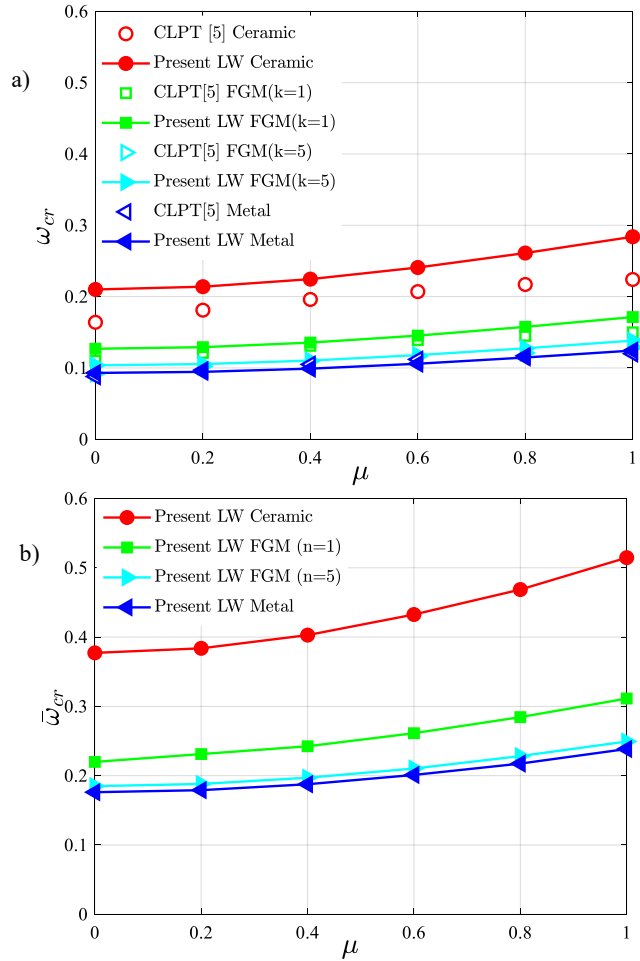


Figure 10. Free vibration frequency for different imperfection amplitude of: a) simply supported plate; b) clamped plate.

CONCLUSIONS

In this paper the finite element solution is derived for the first time, for free vibration analysis of FGM imperfect plates based on layerwise theory of Reddy /25/. An original MATLAB® computer programme is coded for the finite element solution and is used to study effects of various parameters on free vibration response. The following conclusions may be derived:

- 1) The free vibration frequency of FGM plate shows monotonic decrease with increase of side to thickness ratio a/h and aspect ratio b/a . This decrease is more pronounced for thick plates $a/h < 20$ and plates with $b/a < 2$. As thinner the plate is, so are softer the plate and are lower the free vibration frequencies.

- 2) Also, as greater the volume fraction index n is, the less is the ceramic constituent, and consequently the vibration frequency.
- 3) The vibration frequency of imperfect plate is greater than for perfect plate and monotonically increases with increase of imperfection amplitude μ .
- 4) The increase of imperfection amplitude is influenced by the imperfection form. The thick ceramic plate shows higher sensitivity to global-type imperfection forms compared to local-type imperfection forms.
- 5) The free vibration frequency of imperfect plate with clamped edges is greater than with simply supported edges, due to enhanced plate stiffness.

The present finite element solution has shown to be able to include various parameters of importance for free vibration characteristics of FGM plates. Therefore, it may serve for further research of mechanical response of FGM-like structures, under wide variety of different loading, material or geometric parameters.

ACKNOWLEDGEMENT

The authors are thankful for the financial support received from the Ministry of Science, Technological Development and Innovation, Republic of Serbia, grant number 200092.

REFERENCES

1. Chopra A.K., Dynamics of Structures: Theory and Applications to Earthquake Engineering, 6th Ed., Pearson Education Limited, 2024.
2. Sassi, S., Ostiguy, G.L. (1994), *Analysis of the variation of frequencies for imperfect rectangular plates*, J Sound Vibr. 177(5): 675-687. doi: 10.1006/jsvi.1994.1460
3. Chen, C.S., Hsu, C.Y. (2007), *Imperfection sensitivity in the nonlinear vibration oscillations of initially stressed plates*, Appl. Math. Comput. 190(1): 465-475. doi: 10.1016/j.amc.2007.01.069
4. Fung, C.P., Chen, C.S. (2006), *Imperfection sensitivity in the nonlinear vibration of functionally graded plates*, Eur. J Mech. A/Solids, 25(3): 425-436. doi: 10.1016/j.euromechsol.2006.01.003
5. Chen, C.S., Tan, A.H. (2007), *Imperfection sensitivity in the nonlinear vibration of initially stresses functionally graded plates*, Compos. Struct. 78(4): 529-536. doi: 10.1016/j.compstruct.2005.11.014
6. Yang, T., Hu, Y. (2025), *Nonlinear dynamic analyses of a rotating ferromagnetic functionally graded cylindrical shell with initial geometric imperfections*, Thin-Walled Struct. 213: 113264. doi: 10.1016/j.tws.2025.113264
7. Gupta, A., Talha, M. (2016), *An assessment of a non-polynomial based higher order shear and normal deformation theory for vibration response of gradient plates with initial geometric imperfections*, Compos. Part B: Eng. 107: 141-161. doi: 10.1016/j.compositesb.2016.09.071
8. Schneider, W., Timmel, I., Höhn, K. (2005), *The conception of quasi-collapse-affine imperfections: A new approach to unfavourable imperfections of thin-walled shell structures*, Thin-Wall. Struct. 43(8): 1202-1224. doi: 10.1016/j.tws.2005.03.003
9. Guo, L., Zhao, S., Guo, Z., et al. (2026), *Functionally graded engineering structures: An overview*, Eng. Struct. 351: 121995. doi: 10.1016/j.engstruct.2025.121995
10. Xue, Y., Jin, G., Ding, H., Chen, M. (2018), *Free vibration analysis of in-plane functionally graded plates using a refined plate theory and isogeometric approach*, Compos. Struct. 192: 193-205. doi: 10.1016/j.compstruct.2018.02.076
11. Hung, P.T., Thai, C.H., Phung-Van, P. (2023), *Isogeometric bending and free vibration analyses of carbon nanotube-reinforced magneto-electric-elastic microplates using a four variable refined plate theory*, Comp. Struct. 287: 107121. doi: 10.1016/j.compstruct.2023.107121
12. Lieu, Q.X., Lieu, Q.M., Nguyen, T.T. (2026), *Reduced-order isogeometric model in state space for damped vibration and dynamic analyses of functionally graded plates supported by Visco-Winkler-Pasternak foundation*, Compos. Struct. 377: 119877. doi: 10.1016/j.compstruct.2025.119877
13. Izadi, M., Abedi, M., Valvo, P.S. (2024), *Free vibration analysis of a functionally graded porous triangular plate with arbitrary shape and elastic boundary conditions using an isogeometric approach*, Thin-Wall. Struct. 205(Part B): 112422. doi: 10.1016/j.tws.2024.112422
14. Viet Hoang, V.N., Thanh, P.T. (2024), *A new trigonometric shear deformation plate theory for free vibration analysis of FGM plates with two-directional variable thickness*, Thin-Wall. Struct. 194(Part B): 111310. doi: 10.1016/j.tws.2023.111310
15. Foroughi, M., Azhari, M., Sarrami, S., Foroughi, H. (2025), *Free vibration and stability analyses of functionally graded plates resting on elastic foundations based on 2D and quasi-3D shear deformation theories using the finite strip method*, Thin-Wall. Struct. 206: 112715. doi: 10.1016/j.tws.2024.112715
16. Zhao, Y., Qin, B., Wang, Q., Liang, X. (2022), *A unified Jacobi-Ritz approach for vibration analysis of functionally graded porous rectangular plate with arbitrary boundary conditions based on a higher-order shear deformation theory*, Thin-Wall. Struct. 173: 108930. doi: 10.1016/j.tws.2022.108930
17. Demirhan, P.A., Taskin, V. (2019), *Bending and free vibration analysis of Levy-type porous functionally graded plate using state space approach*, Compos. Part B: Eng. 160: 661-676. doi: 10.1016/j.compositesb.2018.12.020
18. Ye, W., Liu, J., Zhang, J., et al. (2021), *A new semi-analytical solution of bending, buckling and free vibration of functionally graded plates using scaled boundary finite element method*, Thin-Wall. Struct. 163: 107776. doi: 10.1016/j.tws.2021.107776
19. Katili, I., Batoz, J.-L., Maknun, I.J., Katili, A.M. (2021), *On static and free vibration analysis of FGM plates using an efficient quadrilateral finite element based on DSPM*, Compos. Struct. 261: 113514. doi: 10.1016/j.compstruct.2020.113514
20. Katili, I., Batoz, J.-L., Widyatmoko, S., Naceur, H. (2024), *The Q4_s plate finite element for three-layer FGM sandwich plates in deflection, stresses, vibration, and thermal buckling analysis*, Compos. Struct. 338: 118098. doi: 10.1016/j.compstruct.2024.118098
21. Belarbi, M.-O., Karamanli, A., Benounas, S., Daikh, A.A. (2025), *Bending, free vibration and buckling finite element analysis of porous functionally graded plates with various porosity distributions using an improved FSDT*, Mech. Based Des. Struct. Mach. 53(1): 401-445. doi: 10.1080/15397734.2024.2366530
22. Assas, T., Bourezane, M., Chenafi, M. (2024), *Static, free vibration, and buckling analysis of functionally graded plates using the strain-based finite element formulation*, Arch. Appl. Mech. 94: 2243-2267. doi: 10.1007/s00419-024-02635-0
23. Assas, T., Bourezane, M., Chenafi, M., Tati, A. (2025), *Static and free vibration response of FGM plates using higher order shear deformation theory and strain-based finite element formulation*, Mech. Based Des. Struct. Mach. 53(4): 3044-3073. doi: 10.1080/15397734.2024.2418828
24. Pham, V.V., Nguyen, V.C., Hadji, L., et al. (2024), *A comprehensive analysis of in-plane functionally graded plates using improved first-order mixed finite element model*, Mech. Based Des. Struct. Mach. 52(8): 5040-5070. doi: 10.1080/15397734.2023.2245876

25. Reddy, J.N., Barbero, E.J., Teply, J.L. (1989), *A plate bending element based on a generalized laminated plate theory*, Int. J. Num. Meth. Eng. 28(10): 2275-2292. doi: 10.1002/nme.1620281006
26. Yildizel, S.A., Tayeh, B.A., Calis, G. (2020), *Experimental and modelling study of mixture design optimisation of glass fibre-reinforced concrete with combined utilisation of Taguchi and Extreme Vertices Design Techniques*, J Mater. Res. Technol. 92 (2): 2093-2106. doi: 10.1016/j.jmrt.2020.02.083
27. Deng, Z., Li, W., Dang, W., et al. (2023), *Multifunctional asphalt concrete pavement toward smart transport infrastructure: Design, performance and perspective*, Compos. Part B: Eng. 265: 110937. doi: 10.1016/j.compositesb.2023.110937
28. Četković, M., Vuksanović, Dj. (2009), *Bending, free vibrations and buckling of laminated composite and sandwich plates using a layerwise displacement model*, Compos. Struct. 88(2): 219-227. doi: 10.1016/j.compstruct.2008.03.039
29. Cetkovic, M. (2022), *Influence of initial geometrical imperfections on thermal stability of laminated composite plates using layerwise finite element*, Compos. Struct. 291: 115547. doi: 10.1016/j.compstruct.2022.115547
30. Matsunaga, H. (2008), *Free vibration and stability of functionally graded plates according to a 2-D higher-order deformation theory*, Compos. Struct. 82(4): 499-512. doi: 10.1016/j.compstruct.2007.01.030
31. Gupta, A., Talha, M. (2016), *An assessment of a non-polynomial based higher order shear and normal deformation theory for vibration response of gradient plates with initial geometric imperfections*, Compos. Part B. Eng. 107: 141-161. doi: 10.1016/j.compositesb.2016.09.071

© 2026 The Author. Structural Integrity and Life, Published by DIVK (The Society for Structural Integrity and Life 'Prof. Dr Stojan Sedmak') (<http://divk.inovacionicentar.rs/ivk/home.html>). This is an open access article distributed under the terms and conditions of the [Creative Commons Attribution-NonCommercial-NoDerivatives 4.0 International License](#)